HYDROCHEMISTRY OF THE UPPER MIOCENE-PLIOCENE-QUATERNARY AQUIFER COMPLEX OF JIFARAH PLAIN, NW-LIBYA

Nawal AL FARRAH, Kristine MARTENS & Kristine WALRAEVENS

(17 figures, 2 tables)

Laboratory for Applied Geology and Hydrogeology, Ghent University, Krijgslaan 281 S8, 9000, Ghent, Belgium.
E-mail: Nawalr2003@yahoo.com; Kristine.Martens @ugent.be; Kristine.Walraevens@ugent.be

ABSTRACT. Large increases in water demand with very little recharge have strained Libya's groundwater resources resulting in serious declines in water levels and quality, especially along the Mediterranean coast where most of the domestic, industrial and agricultural activities are concentrated. The rapid economic expansion, coupled with sharp population growth, in the Jifarah Plain comprising Tripoli, NW-Libya, has created an immediate need for proper groundwater reserves, not only to meet the increasing population's demands, but also to secure a contingency plan. The main problem is salinization of freshwater. Based on the available hydrogeological and hydrochemical information, the sources of salinization are identified. The overpumping for groundwater contributed to the deterioration of the water quality by seawater intrusion and exposing the deep saline water. Cl⁻ is the major pollutant of the aquifer. Water samples were collected from 134 sampling wells in the study area and analyzed for the major cations and anions. The chemical results for the groundwater samples in the plain are classified according to the Stuyfzand groundwater classification system. The water type is mostly CaCl, NaCl and Ca/MgMix. These water types indicate that groundwater chemistry is changed by cation exchange reactions during the mixing process between freshwater and seawater. The majority of groundwater samples (80%) show a composition that is indicative of seawater intrusion.

KEYWORDS: seawater intrusion, overexploitation, upper aquifer, Jifarah Plain, Tripoli, Libya.

1. Introduction

The delicate exploitation of a coastal aquifer usually induces problems of quantity and quality (El Mansouri et al., 2003). Salinization is the most widespread form of groundwater contamination, especially in coastal aquifers, and is represented by the increases of total dissolved solids (TDS) and some specific chemical constituents such as Cl⁻, Na⁺, Mg²⁺, and SO₄²⁻ (Nadler et al., 1981; Magaritz & Luzier, 1985; Dixon & Chiwell, 1992; Morell et al., 1996; Sukhija et al., 1996; Gime´nez & Morell, 1997). Potential salinization sources are diverse, including natural saline groundwater, halite dissolution, seawater intrusion, oil and gas-field brine, domestic, agricultural and industrial effluents, and road salts. Among these sources, seawater intrusion is the most common and widespread in coastal areas, and forces the abandonment of water wells in many instances (Demirel, 2004; Duque et al., 2008; Frohlich et al., 2008; Gaaloul et al., 2003). In many cases, difficulties arise when aquifers are pumped at rates exceeding their natural capacity to transmit water, thus inducing seawater to be drawn into the system to maintain the regional groundwater balance. Problems can also occur when excessive pumping at individual wells lowers the potentiometric surface locally and causes upconing of the natural interface between freshwater and saline water. In order to assess the influence of seawater on a coastal aquifer, it is essential to elucidate the source(s) of salinity and to understand the hydraulic and

hydrogeochemical conditions (Mahesha & Nagaraja, 1996).

The study area covers the coastal part of the Jifarah Plain in NW of Libya (Fig. 1). The Jifarah Plain is a flat area of triangle shape of about 20,000 km². It is bordered by the Mediterranean Sea in the North, the Tunisian border in the West and Jebal Naffusah border in the South and East. The studied coastal area is a coastal strip of around 105 km length and 18 km wide in the North of central Jifarah, where more than 50% of the country's population are concentrated. The climate of the region is semi-arid, typically Mediterranean, with irregular annual rainfall; the average annual precipitation is around 250 mm. Jifarah coastal area, like all Mediterranean coastal regions, has experienced considerable periods of drought during the last two decades. The resulting water deficit was compensated through an increased withdrawal from aquifers. However, aquifers close to coastal areas are the most threatened as they are marked by a very strong borehole density resulting from an intense overexploitation, and show an increase in the mineralization of their waters (DGR, 1995). This constitutes a limiting factor for their use. The Jifarah Plain has long been used for agriculture, and in the past, groundwater has hardly been exploited for irrigation. Recently, the population of the region has increased significantly, following remarkable economic development in sectors such as agro-food, chemistry and oil industry. In addition, various projects related to
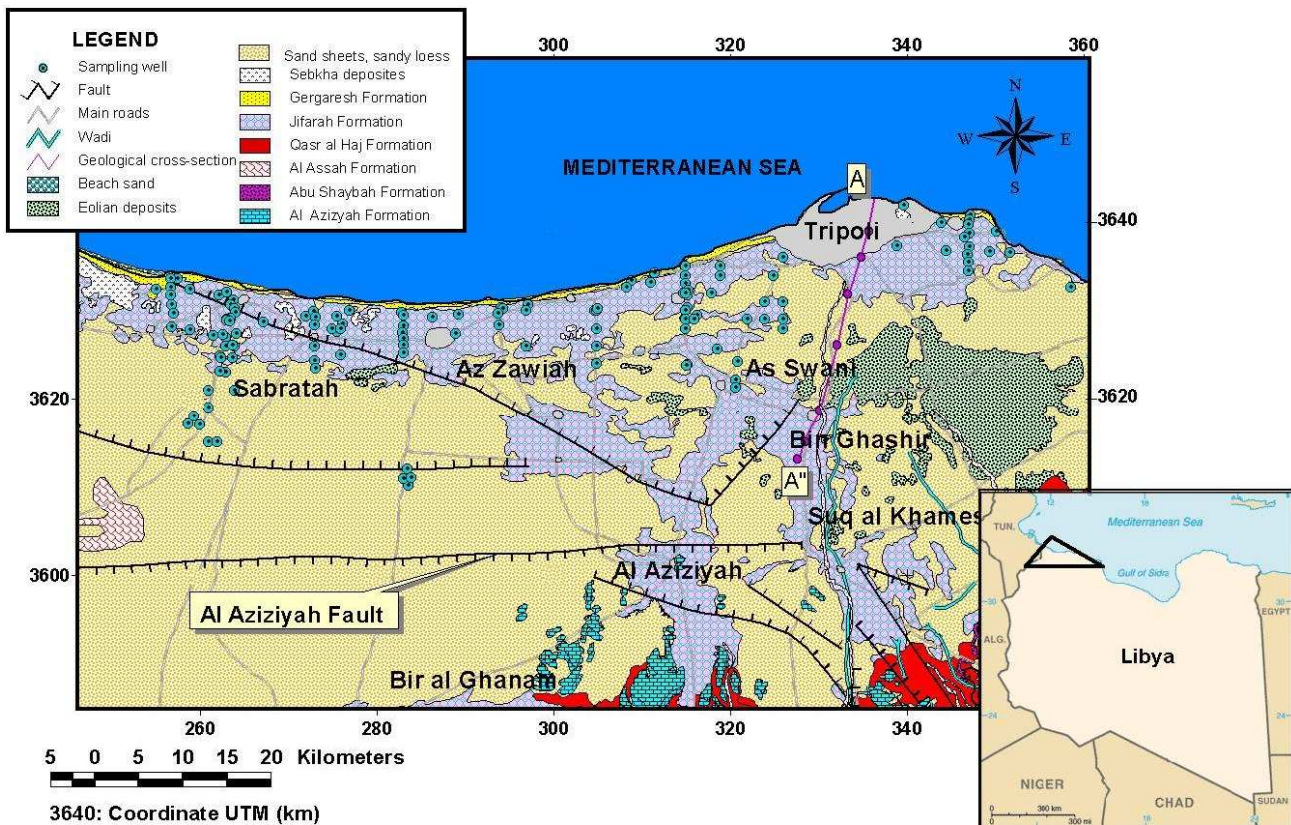
Figure 1. Location and general geological map of the study area.

agriculture and aquaculture have been set up in the plain since the Revolution in 1969.

Different methods have been used to study groundwater salinization and pollution. Generally, fresh groundwater that is not affected by pollution is characterized by low values of EC (electrical conductivity) and a $CaHCO_3$ water type. The latter represents freshwater that has recently infiltrated, while the EC shows a gradual increase from the upland recharge areas towards the lowland discharge areas. Along the coastline, high values of EC are usually attributed to salinization by seawater intrusion (Stamatis & Voudouris, 2003). This paper describes the properties and processes that control the groundwater quality in the Upper Miocene-Pliocene-Quaternary aquifer of the coastal area in central Jifarah, leading to the possible sources of salinity. Groundwater chemistry data from the aquifer have been examined to determine the geochemical conditions and processes that occur in this area and assess their implications for aquifer susceptibility.

2. Geological and hydrogeological setting

The sediments of the Jifarah Plain have been deposited since early Mesozoic times in a near shore lagoonal environment. Structurally, the plain is dominated by EW faults. The block faulting and the near shore environment result in a pronounced change in lithology, laterally as well as vertically. Furthermore, the main faulting system of the Jifarah Plain plays an important role in the hydrogeology of the plain, by placing side by side the

Upper Cretaceous and Tertiary water bearing formations and the great Triassic aquifer (Pallas, 2006).

Figure 1 represents the location and the general geological map for central Jifarah. The geological substratum, which is playing a role in the hydrogeology of the plain, comprises the Middle Triassic (Al Aziziyah Formation, consisting mainly of bedded limestone) and the Upper Triassic (Abu Shaybah Formation, consisting of continental sandstone). All post-Triassic formations have been eroded prior to the Miocene sedimentation. As a consequence, the Miocene, that covers about two thirds of the coastal plain, overlays the Abu Shaybah deposits directly. An exception is found in some small down-faulted blocks south west of Al Aziziyah area where the Lower Cretaceous Kiklah Sandstone and the Upper Cretaceous Ayn Tobi Limestone have been found in some locations. East and South of Tripoli, the whole series from Miocene to Quaternary is made up of clayey sandstone with clay lenses intercalated at various depths; the lower clayey unit is lacking and the Lower Miocene aquifer is in hydraulic continuity with the sandstone formation of Abu Shaybah (Fig. 2).

Figure 2 represents a simplified hydrogeological cross section through the Jifarah Plain. The principal aquifer used by the population in the Jifarah Plain is the Upper Miocene-Pliocene-Quaternary aquifer system, called "first aquifer" or "shallow aquifer" or "upper aquifer"; intercalated thin clayey sand and marl series are dividing the aquifer into a number of horizons, all are considered as one unconfined unit. It is separated from the lower

aquifers by Middle Miocene clay. The upper aquifer is made up of a series of formations of uncertain age. Al Assah Formation is silt, sand and gravels with local occurrences of crystallized gypsum and belongs to the Pliocene- Quaternary deposits; it covers extensive parts of western Jifarah and only a small part is represented in the studied central Jifarah.

The Pleistocene formations include terraces, which consist of cemented gravel and conglomerate. Qasr Al Haj Formation is mainly alluvial fans and cones consisting of clastic materials derived from the scarp. Jifarah Formation consists mainly of fine materials, mostly silt and sand, occasionally with gravel caliche bands and gypsum; it covers extensive parts of the Jifarah Plain. Gergaresh Formation, which is known as Gergaresh Sandstone of Tyrrhennian age, occasionally contains silt lenses and sandy limestone.

The Holocene deposits include recent wadi deposits; these deposits consist of loose gravels and loam varying in thickness from 0.5 to 2 m. Beach sands are represented by a narrow strip at the coast and are made up of shell fragments with a small ratio of silica sands. Eolian deposits (sand dunes) are represented by sand dunes and sheets covering large areas in the Jifarah Plain (field dunes) as well as patches of the coastal strip (coastal dunes). The coastal dunes consist of shell fragments with small amounts of silica sands. It is worth mentioning that the eolian material composing both field dunes and coastal dunes contains a large amount of grains of gypsum. In

some places, it is composed of nearly pure gypsum (98%) especially in the immediate vicinity of the sebkhas, with a silty gypsum filling (IRC, 1995). Fluvial–eolian deposits are found on the plateau surface in central Jifarah. They are made up of silt, clay and fine sands with occasional caliche bands. Sebkha sediments are observed along the coastal area of the plain. They occupy the relatively low topographic areas and are separated from the sea by sea cliffs. Some of the sebkhas have occasional incursions of the sea and others may have subsurface connection with the seawater. Most of them are marked by the presence of scattered sand islands.

In central Jifarah, the lithology of the upper aquifer varies widely and includes limestone, gravel, marl, clay, sand and sandstone. Between Sabratah and Bir al Ghanam the lower part of the upper aquifer consists of gypsiferous limestone and gypsiferous sandstone. The depth to the bottom of the upper aquifer varies between 30-200 m and depths of the wells that are utilizing this aquifer are between 30-180 m. Most of the wells tapping this aquifer give productivity of about 20-80 m^3/hr.

3. Methodology

3.1 Groundwater sampling and analysis

This study assesses the quality of groundwater from 134 different borehole locations in the coastal area of the plain. The methods employed for this study are field
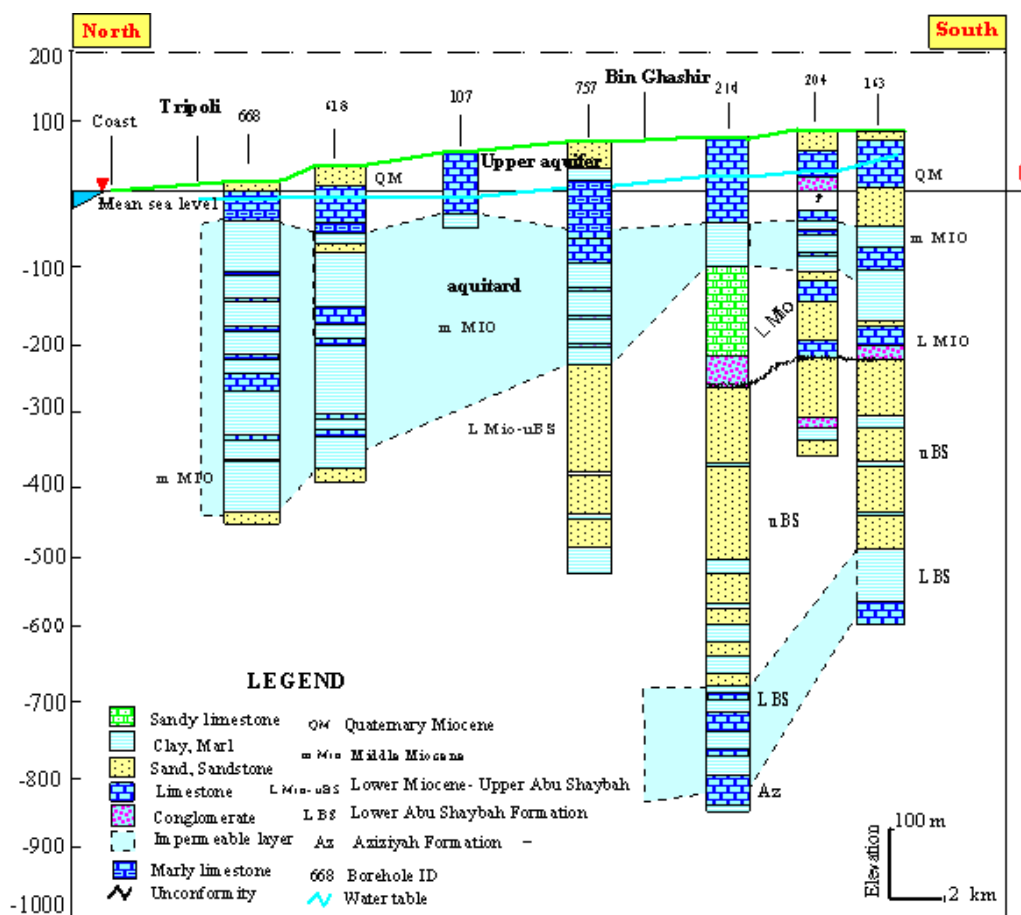

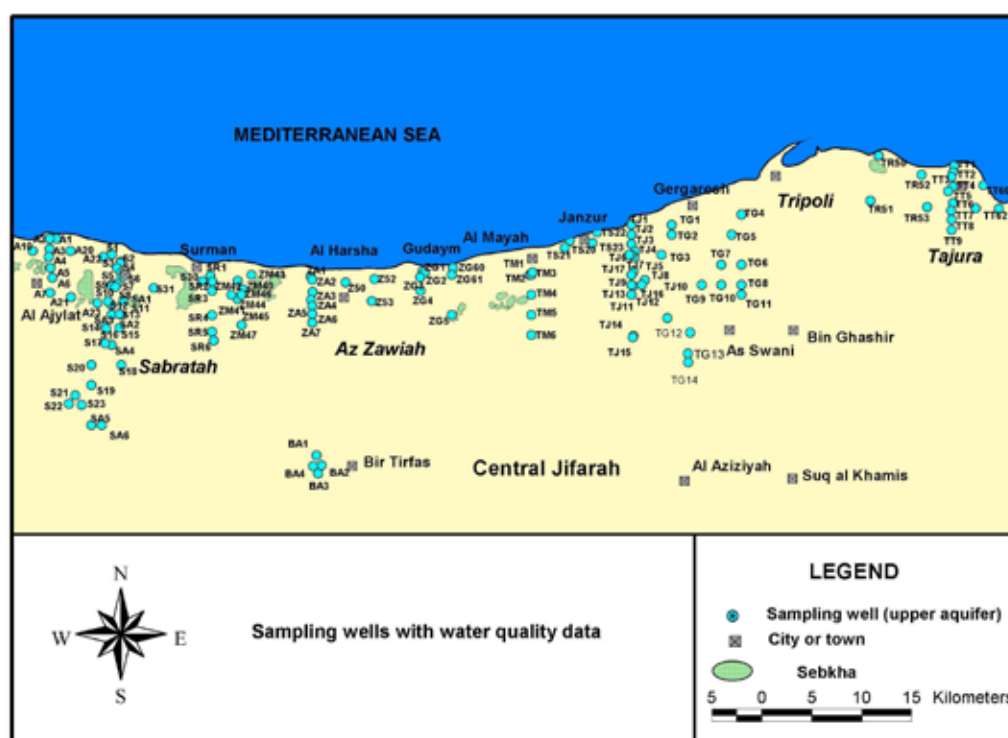**Figure 2**. Hydrogeological cross section A-A" through the Jifarah Plain.

measurements, sampling and laboratory analysis. The regional hydrogeochemical survey and the water level measurements were performed during dry periods from March to July in 2007 and from September to November of 2008. It must be underlined that the Jifarah Plain is a semi arid to arid region with only trace precipitation, where drought can prevail for several years; the annual average precipitation of 250 mm mostly occurs in December and January. In the coastal area, a total of 134 shallow and deep wells (mostly 30-180 m deep), located at different distances from the Mediterranean Sea, were selected for groundwater sampling and water level measurement across the major cities (Fig. 3). 134 water samples were collected from the 134 sampling wells in the study area and analyzed for the major cations and anions. The samples were collected during pumping and the water level measurements were performed in static condition.

The sampling points were chosen along vertical lines perpendicular to the coast, with lengths comprised between 8 and 28 km, in order to explore the aquifer from inland to the coast line. The collected water samples were preserved in polyethylene bottles after filtering on 0.45 µm cellulose membrane filters. Two samples were taken from each well, one for determining anions, the other for determining cations. Samples for cation analysis were acidified to lower the pH to around pH = 2 by adding a few drops of ultra-pure nitric acid. Parameters measured are physical properties such as: water depth, pH, temperature, water level and electrical conductivity (EC). Chemical parameters analyzed are: sodium (Na^+), potassium (K^+), calcium (Ca^{2+}), magnesium (Mg^{2+}), iron (Fe^{Total}), manganese (Mn^{2+}), chloride (Cl^-), nitrate (NO_3^-), sulphate (SO_4^{2-}), bicarbonate (HCO_3^-), carbonate (CO_3^{2-}) and phosphate (PO_4^{3-}). Water level was measured from

the ground surface using water level meter, and pH was analyzed using a pH meter and glass electrode. Cations (Na^+, K^+, Mn^{2+}, Fe^{Total}, Ca^{2+}, Mg^{2+}) were analyzed using Flame Atomic Absorption Spectrometry (Varian Zeeman Spectra AA 400). Si (for 7 samples) was analysed by using Furnace Atomic Absorption Spectrometry with electrothermal atomisation in a graphite furnace (Varian Zeeman Graphite tube Spectra AA 400). Zn (for 7 samples) was determined by using Varian Spectrometer AA 400 with ACT-80 atom concentrator tube with air and acetylene gas. Anions (Cl^-, NO_3^-, NO_2^-, and PO_4^{3-}) and NH_4^+ were analysed using the Molecular Absorption Spectrophotometer (UV-VIS spectrophotometer Shimadzu UV mini 1240-Heatingplate 105°C). SO_4^{2-} was determined with a turbidimetric method and F^- (for 7 samples) with ion selective electrode. Determination of bicarbonate (HCO_3^-) and carbonate (CO_3^{2-}) used the titration method with dilute HCl acid. This method measures bicarbonate (HCO_3^-), carbonate (CO_3^{2-}) and alkalinity levels in water. The above mentioned analytical methods for the major ions were used for the samples analyzed at the Laboratory of Applied Geology and Hydrogeology, Ghent University, and were provided in the Laboratory Manual and in Standard Methods for Examination of Water and Wastewater (APHA, 1985). Careful quality controls were undertaken for all samples to obtain a reliable analytical dataset with an ionic balance error less than 5%.

3.2 Hydrochemical interpretation methods

The interpretation process is mainly based on water type classification according to Stuyfzand (1986), graphical illustration methods including Piper diagram, calculation of ionic ratios, and elaboration of maps and cross-sections showing the spatial and vertical distribution of water

LEVEL Number Name	Number of subdivisions	Criterion	Codes
I Main type	6	Cl⁻	F, Fb, B, Bs, S and H
II Type	11	Total hardness	*,0,1,2,3,4,5,6,7,8,9
III Sub-type	54	Most important cation and anion	NaCl, NaSO₄, NaHSO₄, NaMix, KNO₃, NH₄SO₄, CaCl, CaSO₄, CaNO₃, CaHCO₃, CaMix, MgCl, MgHCO₃, MgMix, AlSO₄, FeSO₄.
IV Class	3	[Na+K+Mg] corrected for sea salt	-, ø, +
Where: F = Fresh, Fb = Fresh brackish, B = Brackish, Bs = Brackish saline, S = Saline and H = Hyperhaline			

Table 1. The hierarchical structure of the Stuyfzand classification system (Stuyfzand, 1986).

quality parameters in the study area, to evaluate the sources of salinization.

The Stuyfzand classification (Stuyfzand, 1986, 1993) subdivides the most important chemical water characteristics at 4 levels (Table 1). The first level (main type) is determined based on the chloride content. The second level (type) is determined on the basis of an index for hardness. The third level, classification into subtypes is determined based on the dominant cations and anions. Finally, the class is determined on the basis of the sum of Na^+, K^+ and Mg^{2+} in meq/l, corrected for a sea salt contribution:

{Na + K + Mg} corrected = [Na + K + Mg] measured $-1.061Cl^-$, where: - = Often pointing at a saltwater intrusion, {Na + K + Mg} corrected $<-\sqrt{0.5}$ Cl; + = Often pointing at a freshwater encroachment, {Na + K + Mg} corrected $>\sqrt{0.5}$ Cl; 0 = At an equilibrium, $-\sqrt{0.5}$ Cl $\leq$ {Na + K + Mg} corrected $\leq +\sqrt{0.5}$ Cl

This indicates whether cation exchange has taken place and also the nature of the exchange, by assuming that all Cl^- originates from seawater, that fractionation of major constituents of the seawater upon spraying can be neglected, and that Cl^- behaves conservatively. Each of the subdivisions contributes to the total code (and name) of the water type. "-" code indicates {Na + K + Mg} deficit, "+" code indicates {Na + K + Mg} surplus and "0" code indicates {Na + K + Mg} equilibrium.

{Na + K + Mg} surplus and "0" code indicates {Na + K + Mg} equilibrium.

It is well-known that the hydrogeochemical composition of coastal groundwater affected by seawater intrusion is mainly controlled by cation exchange reactions next to the simple mixing process (Appelo & Postma, 1993). These processes can explain deviations of the concentrations of cations from conservative mixing of both waters. Walraevens & Van Camp (2005) explained the process of freshening and salinization of coastal aquifers with the end members seawater and freshwater. Freshwater is generally conceived as infiltrating rain having dissolved calcite, the water type is $F-CaHCO_3 0$, whereas seawater type is $S-NaCl 0$ according to the classification of Stuyfzand (1986).

Salinization is induced as the new saline end member is introduced into the freshwater aquifer. The main chemical reaction is cation exchange, resulting in deficit of Na^+ and surplus of Ca^{2+}:

$Na^+ + 0.5Ca-X_2 \rightarrow Na-X + 0.5Ca^{2+}$ where X represents the natural exchanger in the reactions. During cation exchange, the dominant Na^+ ions are adsorbed and Ca^{2+} ions released, so that the resulting water moves from NaCl water to CaCl water, which is typical for salinization (Jones et al., 1999, Barker et al., 1998). The salinization process can be schematized as follows (Walraevens & Van Camp, 2005):

$CaHCO_3 0 \Rightarrow CaCl- \Rightarrow NaCl- \Rightarrow NaCl 0$

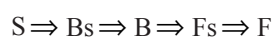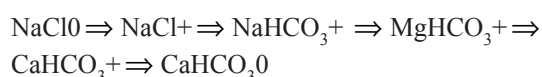$F \Rightarrow Fb \Rightarrow B \Rightarrow Bs \Rightarrow S$
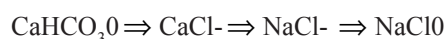
The chloride ion concentration is taken as a reference parameter (Jones et al., 1999). Therefore, as saltwater intrudes coastal freshwater aquifers, the Na/Cl ratio decreases and the Ca/Cl ratio increases.

Upon the inflow of freshwater a reverse process takes place:

$0.5Ca^{2+} + Na-X \rightarrow 0.5Ca-X_2 + Na^+$
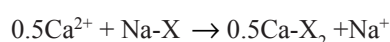
Flushing of the saline aquifer by freshwater will thus result in uptake of Ca^{2+} by the exchanger with concomitant release of Na^+. This is reflected in the increase of the Na/Cl ratio, and formation of the $NaHCO_3$ water type, which is typical for freshening. The anion HCO_3^- is not affected because natural sediments behave as cation exchanger at the usual near-natural pH of groundwater (Appelo, 1994). The freshening process can be schematized as follows (Walraevens & Van Camp, 2005):

$NaCl 0 \Rightarrow NaCl+ \Rightarrow NaHCO_3+ \Rightarrow MgHCO_3+ \Rightarrow CaHCO_3+ \Rightarrow CaHCO_3 0$

$S \Rightarrow Bs \Rightarrow B \Rightarrow Fs \Rightarrow F$

Upstream of the saltwater-freshwater boundary, a sequence of Na^+, Mg^{2+}, and Ca^{2+} dominated water types should be found (Appelo, 1994). The development of a pattern of water types in the mixing of seawater and freshwater depends on the amounts of the exchangeable cations and their concentrations in solution (Appelo & Postma, 1993).
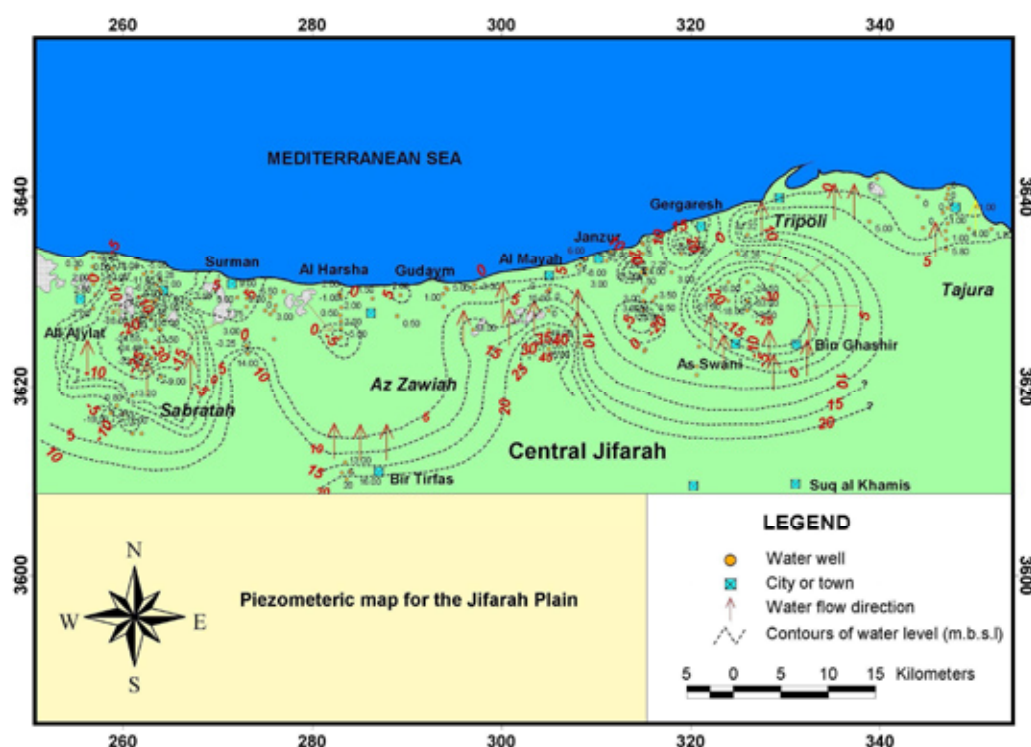
Figure 4. Piezometric map for the coastal area of central Jifarah.

4. Results and discussion

4.1 Piezometry

The overexploitation of the Jifarah upper aquifer is characterized by the falling of piezometric head over a wide region, reducing the outflow rate to the sea, and the continuous degradation of the chemical quality of water. Depression cones in various places have dropped from 25 to 35 m below sea level (Fig. 4), which testifies the inversion of the hydraulic gradient and the intrusion of seawater. This was mainly observed in Sabratah region and southern Tripoli.

4.2 Major hydrochemical parameters

Major anions and cations, pH, conductivity, total dissolved solids, as well as the temperature and colour were assessed on all samples collected. The results show that: temperature ranges between 18 - 26 °C, pH range is 6.71 - 9.94, conductivity between 510 -15,650 µS/cm (25 °C), TDS range 360 - 11,141 mg/l and chloride concentration ranges from 2 - 5285 mg/l. In 61% of samples, Cl^- concentration exceeded the WHO (1984) value for standard drinking water (250 mg/l) and in 26% of samples, Cl^- concentration exceeded the WHO (1984) highest admissible concentration (600 mg/l). This high Cl^- concentration is probably due to mixing with seawater. Characteristics of hydrochemical analytical results are summarised in Table 2.

All geological environments may contain naturally occurring saline water resulting from geochemical processes within each geological setting. Naturally, highly saline waters typically have Cl^- as the dominant anion and Na^+ as the dominant cation. Exceptions are waters

Table 2. Descriptive statistics for physico-chemical parameters of groundwater (in mg/l) in the Jifarah coastal area.

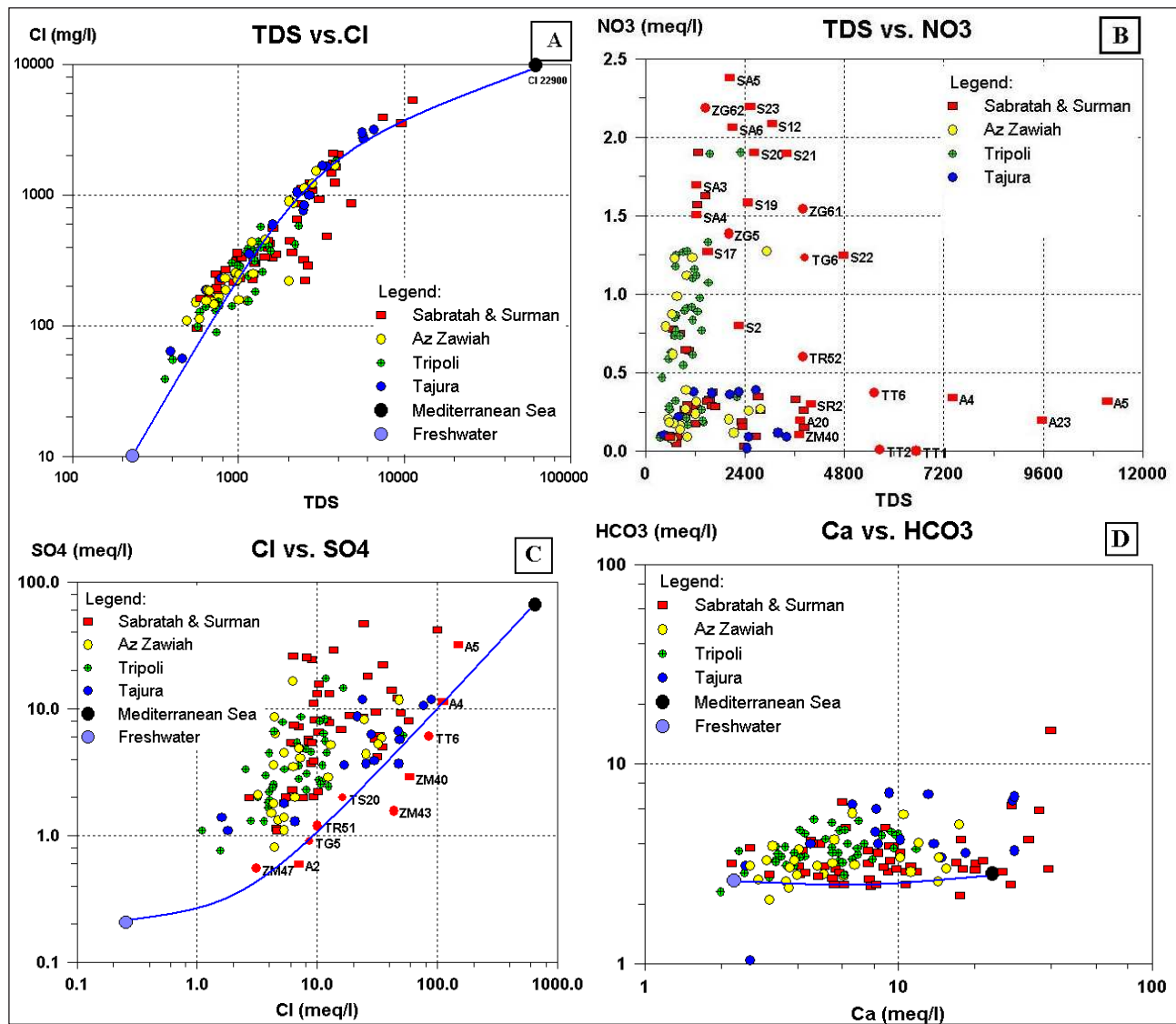| Parameters	Min	Max	Mean
Na^+	12	2748.5	313.9
K^+	0.5	74.3	13.2
Ca^{2+}	40	796.2	182.6
Fe^{2+}	0	1.4	0.085
Mn^{2+}	0	0.004	0.005
Mg^{2+}	8.7	409.4	76.1
NH_4^+	0	0.54	0.02
Cl^-	1.8	5282	627.4
SO_4^{2-}	26.5	2238.4	323.3
HCO_3^-	6.2	897	226.9
NO_3^-	0.2	147.5	40.4
pH	6.7	9.94	-
EC(μS/cm 25°C)	510	15,650	2858.6
T(°C)	18	26	22.9
TDS(mg/l)	359.9	11,141	1818

Figure 5A-D. TDS vs. Cl⁻, TDS vs. NO₃⁻, Cl⁻ vs. SO₄²⁻ and Ca²⁺ vs. HCO₃⁻. The curves represent mixing of freshwater and Mediterranean Seawater.

associated with saline seep and some salt flats, which often have a SO_4^{2-} as a major anion (Kreitler et al., 1993). Figure 5 presents scatter diagrams for TDS vs. Cl⁻, TDS vs. NO_3^-, Cl⁻ vs. SO_4^{2-} and Ca²⁺ vs. HCO_3^- and Figure 6 presents scatter diagrams for major cation concentrations versus the Cl⁻ concentration. An obvious positive correlation can be seen in the case of the TDS vs. Cl⁻ graph (Fig. 5A): a positive increase of Cl⁻ concentration by increasing TDS is observed. This can also be seen in Na⁺ and K⁺ vs. Cl⁻ graphs (Fig. 6C-D). Under conditions of saline intrusion, Na⁺ in seawater replaces Ca²⁺ adsorbed onto the surface of clays. This results in a relative depletion of Na⁺ from seawater, therefore Na⁺ concentrations for most of samples are relatively low and plotted below the mixing curve. For the Ca²⁺ vs. HCO_3^- graph (Fig. 5D), the data from the study region reveal a scattered distribution on the diagram. Random distribution of data indicates the measured samples have different water types, where additional Ca²⁺ is added due to cation exchange during salinization and calcite dissolution. The scatter diagram in Fig. 5B shows high NO_3^- concentrations for many samples

collected from Sabratah area. The highest NO_3^- concentrations were recorded towards the south of Sabratah where the agricultural activity is more intense. In Fig. 5C, a large number of samples are plotted above the seawater-freshwater mixing curve. Apart from the effect of seawater intrusion, the possible extra source of SO_4^{2-} is dissolution of gypsum from the upper aquifer's formation in southern Sabratah. Furthermore, the scattered sebkha deposits produce high SO_4^{2-} waters for several wells. For samples plotting below the mixing curve, SO_4^{2-} reduction is occurring. The positive linear relation between Na⁺, Mg²⁺ and K⁺ versus Cl⁻ in Fig. 6B-D represents mixing of the fresh groundwater with the seawater end member.

Levels of Cl⁻ and EC are the most simple indicators of seawater intrusion or salinization (Mercado, 1985; El Moujabber et al., 2006). In general, the EC, which is tightly linked to TDS, is a measure of salinity, and therefore is generally closely related to the Cl⁻ content. Both of them (EC and Cl⁻) show the same general decrease from the Mediterranean shoreline towards the south.
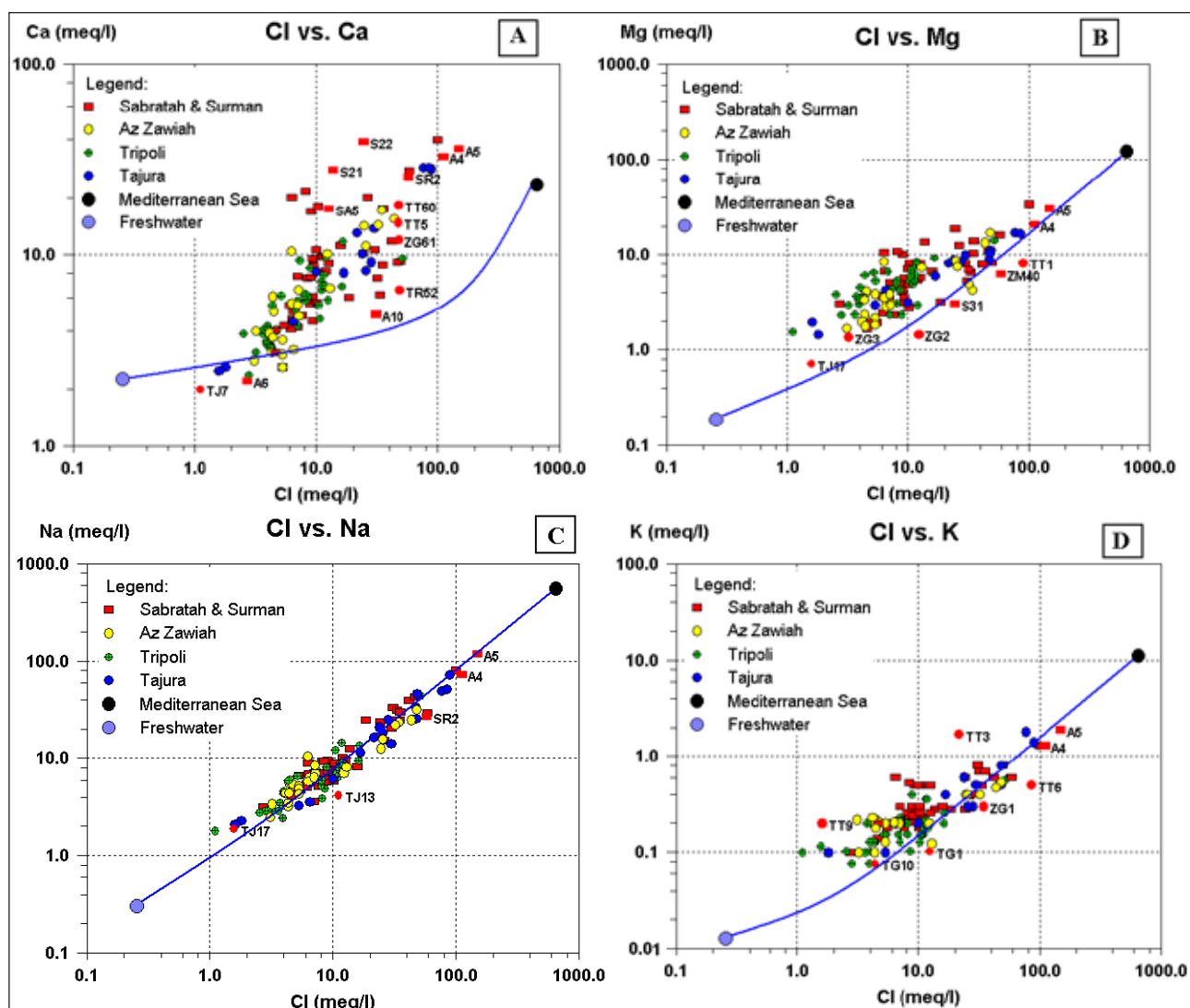
Figure 6A-D. Cl⁻ vs. major cation concentrations. The curves represent mixing of freshwater and Mediterranean Seawater.
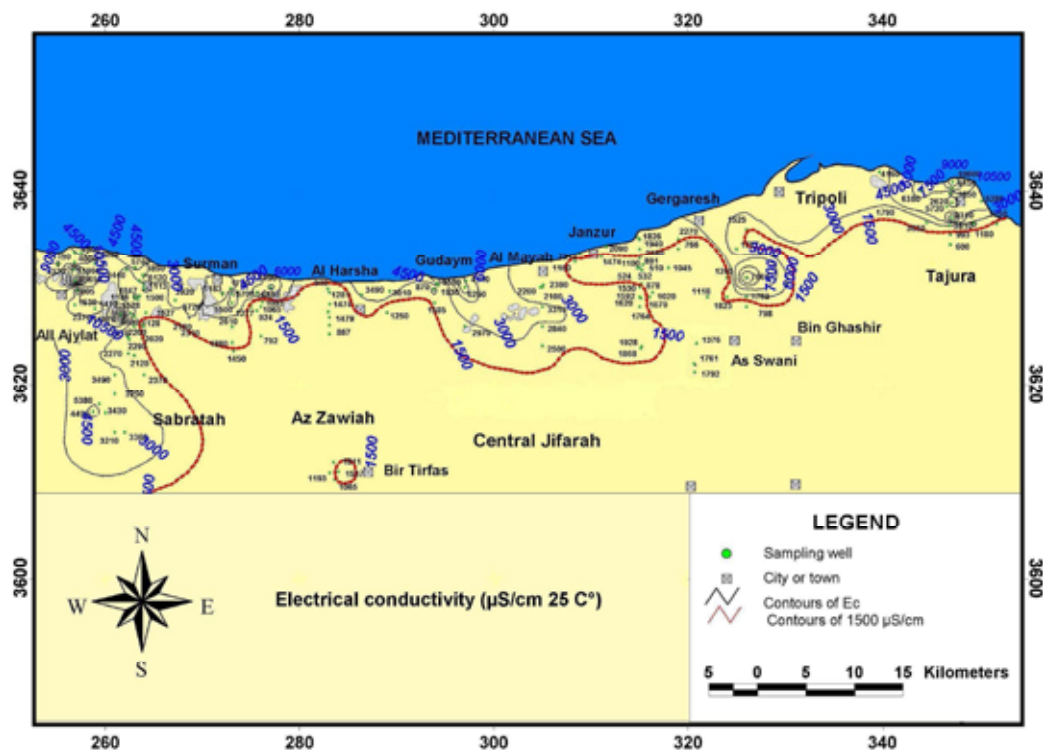

Figure 7. Spatial distribution of groundwater EC in the coastal area of Jifarah Plain.
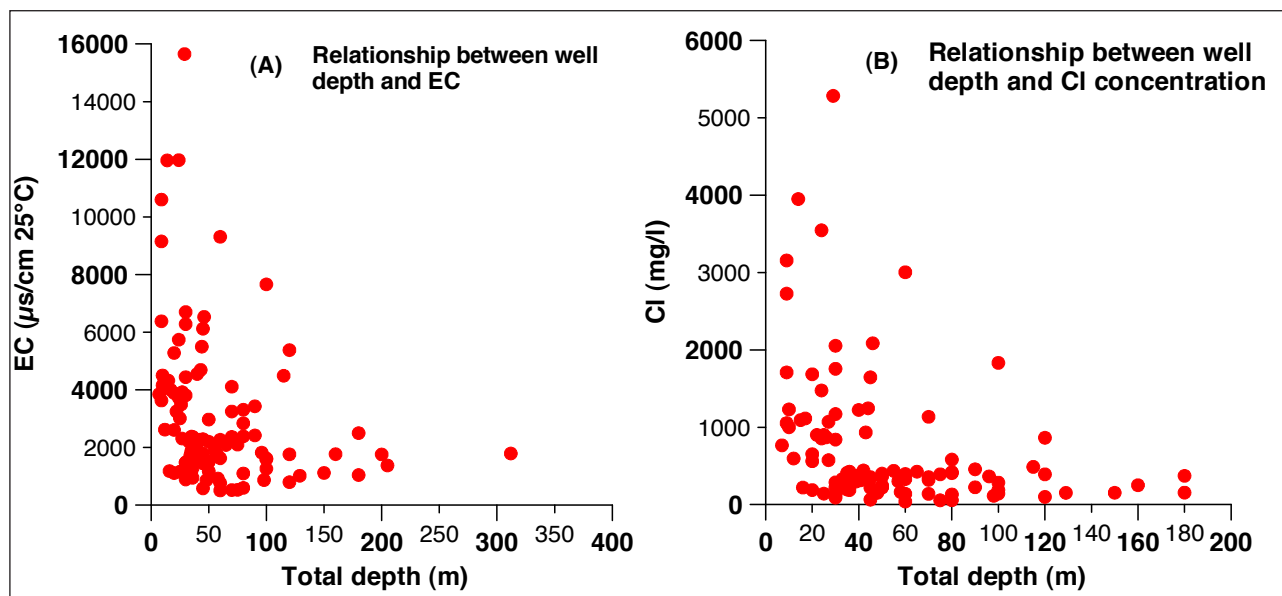
Figure 8A-B. Relationship between well depth, Cl⁻ and EC.

Frequent local increases in both variables are observed at the depression cones as a result of the high pumping rate. The spatial distribution of EC from analyzed groundwater samples across the Jifarah Plain is presented in Figure 7. The salinization of groundwater in the Jifarah Plain leads to a large range in EC; the maximum value of 15,650 µS/cm (25°) is recorded for sample A5 in Al Ajylat area, located at about 4 km south of Sabratah shoreline. In the depression cone of Sabratah, at about 6 km from the Mediterranean Sea, a value of 11,970 µS/cm (25°) is recorded for sample A23 and a value of 11,960 µS/cm (25°) is recorded for sample A4, about 3 km south of Sabratah shoreline. In Az Zawiah area, EC shows low values compared to the other regions, although close to the coast, EC is high, especially at the coast of Gudaym area. In relation to the water level decline, a very

considerable increase of EC has also been recorded in the Tripoli region. This is very clear south of Gergaresh, where the EC indicates a high increase in salinity, coinciding with the cone of depression that formed in As Swani Well field just a few kilometers north of Bin Ghashir. Near to the seaside at Tajura, EC increases clearly to about 10,600 µS/cm (25°). In a few boreholes with high local pumping rate, EC has started to increase even more. Overpumping of the aquifer in the study area leads to migration of the saltwater wedge inland and upconing of deep saline water, resulting in high EC. The local effect of the scattered sebkha deposits additionally contributes to the salinity increase in several wells (i.e. A4, TM5, ZG5, SR3 and A5).

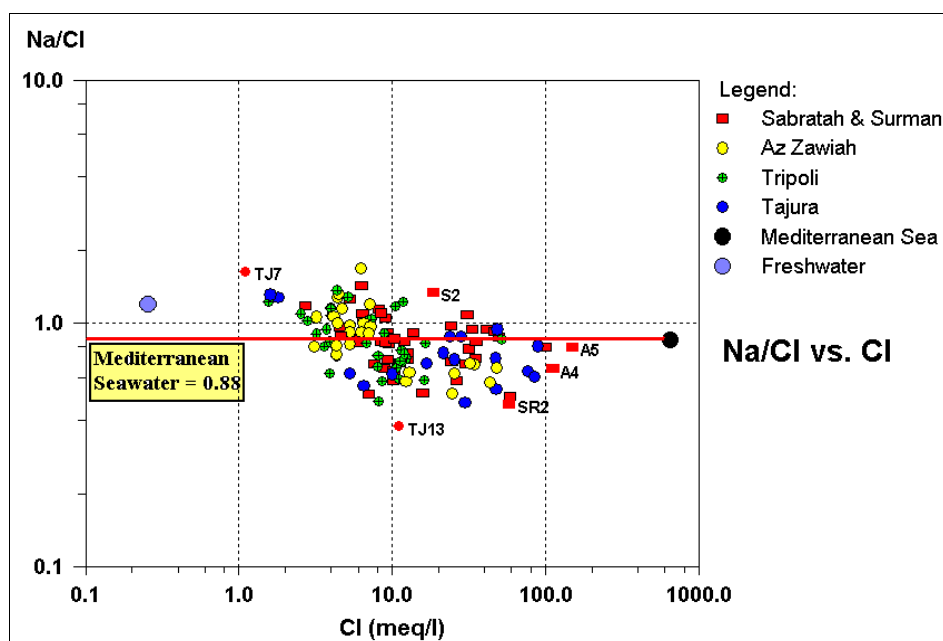In Figure 8, the depths of the wells tapping the coastal aquifer vary because the depth to the fresh water/seawater

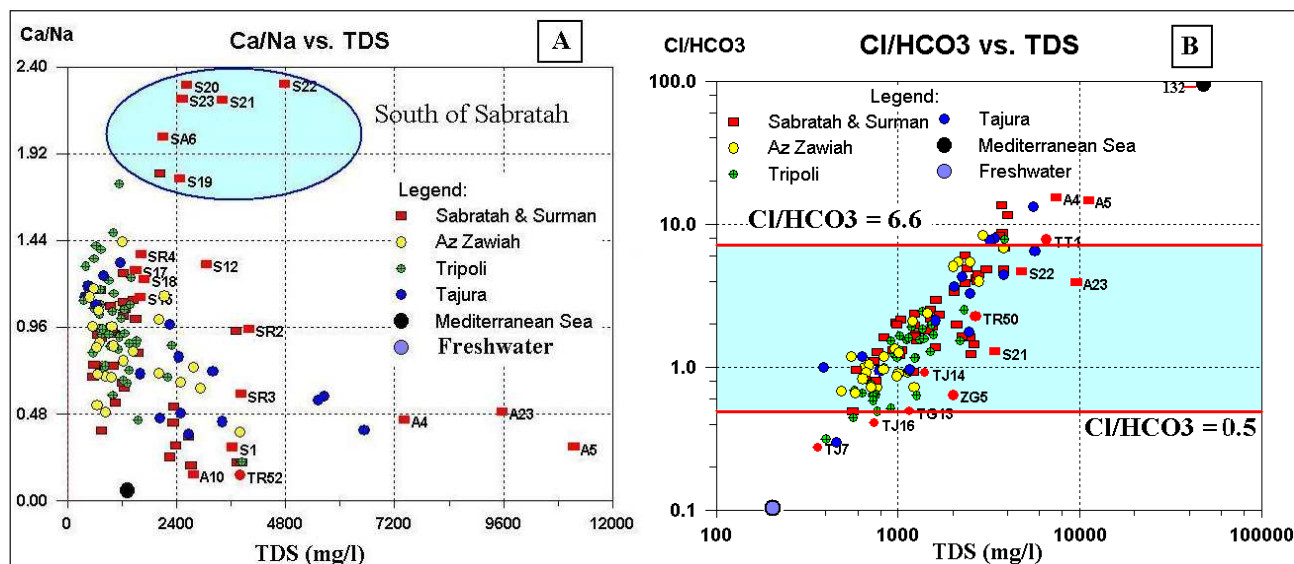

Figure 9. Molar ratio of Na/Cl vs. Cl⁻ concentrations.

Figure 10A-B. Ionic ratios Ca/Na vs. TDS and Cl /HCO$_3$ vs. TDS.

interface varies. Many deeper wells show low Cl⁻ and EC levels, indicating inland sampling wells are least affected by saline waters.

4.3 Major hydrogeochemical processes and groundwater composition

4.3.1 Ionic ratio

Effects of seawater encroachment have been evaluated by studying the ionic ratios. Lower ratios of Na/Cl than seawater values (0.88) indicate seawater encroachment. Conservative seawater–freshwater mixing is expected to show a linear increase in Na⁺ and Cl⁻ (Sanchez Martos et al., 1999). Fig. 9 shows molar ratios of Na/Cl versus Cl⁻ concentrations. The Na/Cl ratios range from 0.38 to 1.68. 74% of groundwater samples were less than or slightly higher than the Mediterranean seawater ratio (0.88). The lowered values with respect to the Mediterranean seawater ratio are resulting from cation exchange occurring when seawater intrudes freshwater aquifers, resulting in the deficit of Na⁺ and surplus of Ca^{2+}.

Another useful ionic ratio is Cl/HCO$_3$. The ratio of Cl/HCO$_3$ ranges between 0.48 and 26.5. The effect of salinization can be classified using the Cl/HCO$_3$ ratio, as follows: <0.5 for unaffected, 0.5–6.6 for slightly and moderately affected and >6.6 for strongly affected
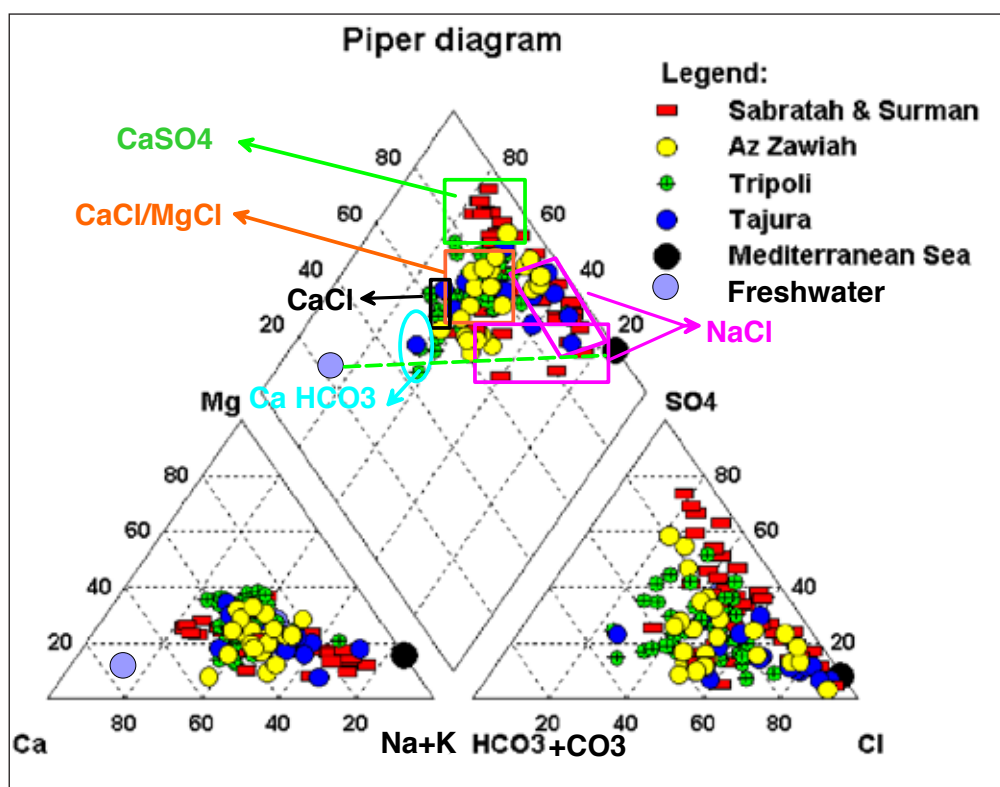

Figure 11. Water types according to Piper diagram.

(Revelle, 1941; Todd, 1959). Considering the values of Cl⁻ concentration and the ratio of Cl/HCO$_3$, 23 % of the groundwaters were strongly affected by the saline water and 77 % were slightly or moderately affected.

Furthermore, to evaluate the effect of seawater mixing and the effect of cation exchange processes qualitatively, we have examined the ionic ratios (Ca/Na and Cl/HCO$_3$) vs. TDS diagrams (Fig. 10). There is a specific trend in the Ca/Na vs. TDS diagram (Fig. 10A), whereby the Ca/Na ratio rises to more than 1.8 for samples collected from southern Sabratah region (i.e. S19, S20, S21, S22, S23 and SA6) suggesting that Ca/Na ratios are controlled by other processes in addition to cation exchange during seawater mixing. Dissolution of gypsum from the lower aquifer in this area contributed to the increase in salinity and is reflected in the higher Ca/Na ratio. In the Cl/HCO$_3$ vs. TDS diagram (Fig. 10B), on the other hand, a positive correlation between the two variables is visible. This trend suggests that high TDS groundwaters are typically enriched in chloride ion, mainly due to seawater mixing.

4.3.2 Groundwater classification

A. Piper diagram

Classification of hydrochemical facies for groundwaters according to Piper diagram is shown in Fig.11. Although various hydrochemical facies were observed, CaCl and NaCl types are dominant. Large proportions of the groundwaters show NaCl type, which generally indicates a strong seawater influence (Pulido-Leboeuf, 2004) or upconing of deep saltwater, while CaCl water type is indicating salinization and cation exchange reaction (Walraevens & Van Camp, 2005). Furthermore, sources of CaSO$_4$ water type are the dissolution of gypsum from the lower aquifer formation (e.g. S18, S19, S20, S21, S22, and S23) and, to some extent, the dissolution of the scattered sebkha deposited (for wells ZG5 and TM5). Furthermore, in the south towards the recharge area,

groundwater of CaHCO$_3$ type is associated to the lowest mineralisation values. This reflects the dissolution of carbonate minerals in carbonate aquifers which make up most of the watershed boundaries. This water type has been observed only to the south of Janzur for samples TJ7, TJ16 and TJ17, for sample TT9 south of Tajura, and TG11 south of Tripoli.

B. Water type classification according to Stuyfzand (1986)

The chemical results for the groundwater samples are classified according to the Stuyfzand (1986) groundwater classification system as follows:

Main type (chloride concentration):
Figure 12 shows the spatial distribution of main water types for all analyzed samples. The study area was divided into four regions according to Main Water Type:
Fresh (F): Cl⁻ < 150 mg/l
Fresh-Brackish (Fb): 150 < Cl⁻ < 300 mg/l
Brackish (B): 300 < Cl⁻ < 1000 mg/l
Brackish-Salt (Bs): 1000 < Cl⁻ < 10,000 mg/l

F water was only found in wells located South of Janzur (i.e. TJ6, TJ7, TJ14, TJ15, TJ16, TJ17, TG3 and TG2), this may be explained by recharge nearby a local high topography area, which refreshes the aquifer and restricts the mixing of fresh and salt water, consequently limiting the degree of salinization. Only 14% from the analyzed samples have F water as a main type. Fb water is observed in 32% of the analyzed samples, it is found in Janzur and Gergaresh to the west of Tripoli. Fb water is also found in Al Harsha area and towards the south for wells in Bir Tirfas such as BA1, BA2, BA3 and BA4. Fb water can also be observed very locally, in many wells in the South of the study area. This water type is expected to be the main type in the south towards the recharge area, where no data exist. Many of the upper aquifer wells
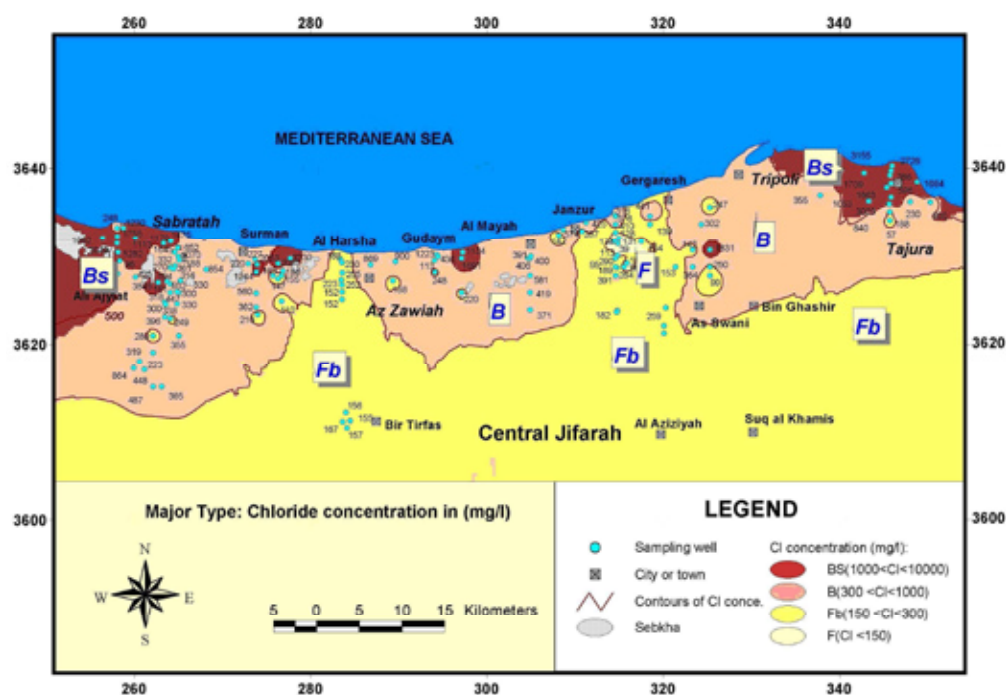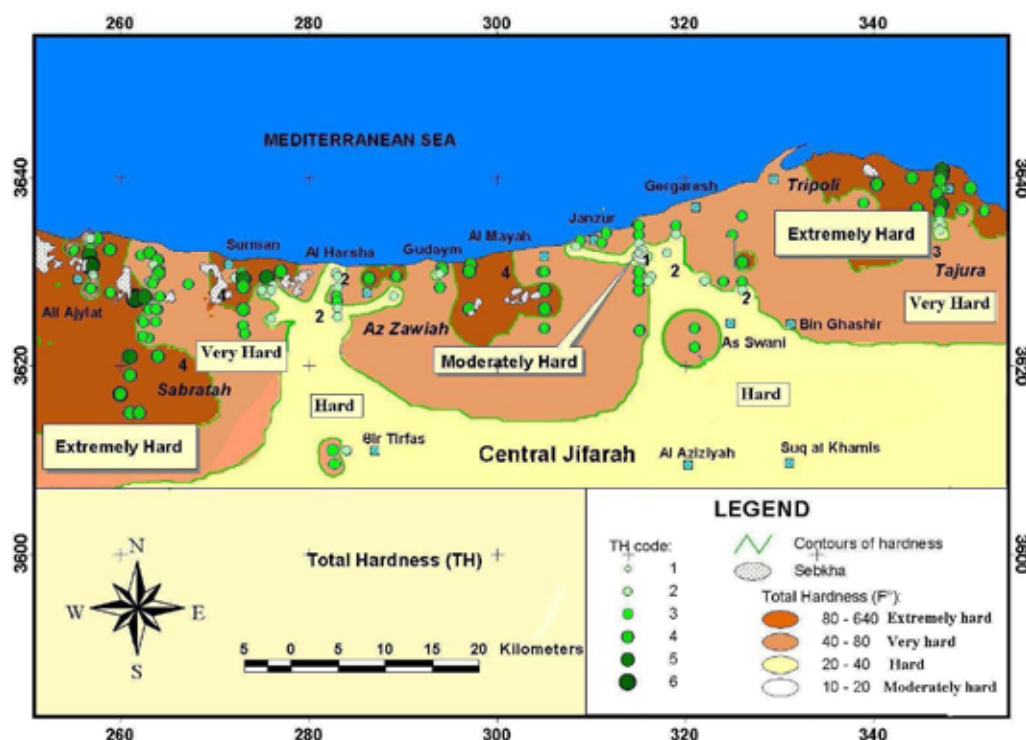

Figure 12. Main water type (chloride concentration).

Figure 13. Water type (Hardness code).

(35%) in the study area have B water. Further eastwards to Tajura, the water becomes Bs for 10 wells, with Cl⁻ concentration more than 1000 mg/l. Bs water is also found locally, near the coast in Gudaym and Surman. Further to the west, Bs water is the main water type for many wells in Sabratah and Al Ajylat.

Type (hardness):
Fig. 13 represents the spatial distribution of water type for the analyzed samples, which reveals increased hardness values towards the coast and in areas, where the local cones of depression were formed. Hardness values range

from 3.16 to 73.42 meq/l (15.80 - 367.09 F°). The study area is divided into four regions according to Water Type (hardness):

Moderately Hard: Total Hardness = 10 - 20 F°
Hard: Total Hardness = 20 - 40 F°
Very Hard: Total Hardness = 40 - 80 F°
Extremely Hard: Total Hardness > 80 F°

It is noticed that 1% of the analyzed water samples is moderately hard, 28% are hard, 43% are very hard, and 28% are extremely hard. It is also noticed that hard water occurs mostly in wells with Fb water in Janzur, Bir Tirfas, Al Harsha and two wells to the south of Tajura, while very
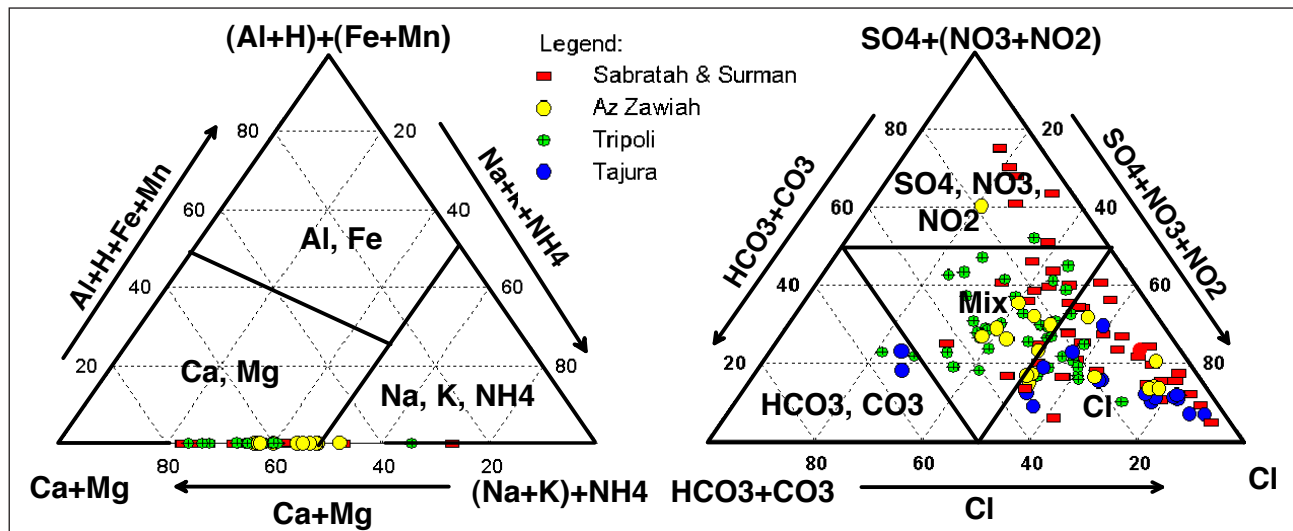

Figure 14. Water class (cation exchange code).
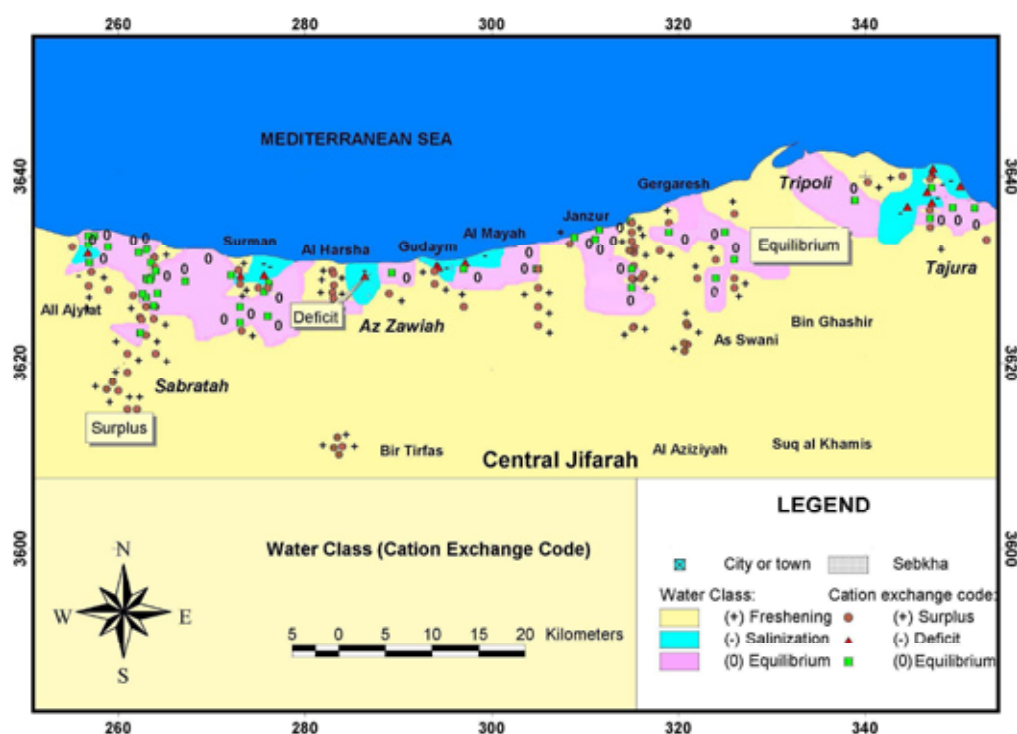
Figure 15. Classification of water subtypes in the Jifarah Plain groundwater according to Stuyfzand (1986).

hard and extremely hard waters occur in B and Bs waters in the middle, western and eastern part of the study area. Moderately hard water was only found in two wells in Janzur, where the main water type was classified as F. For example, wells TJ7 and TJ17 have F water with Cl⁻ less than 150 mg/l and total hardness between 10 and 20 F°; well SA1 has Fb water with total hardness between 20- 40 F° (hard water); wells A23 and S10 have B very hard and Bs extremely hard waters, respectively. This means that, overall, F water is moderately hard; Fb water is very hard to hard; B water is very hard and Bs water is extremely hard.

Class (cation exchange code):
Fig. 14 represents the spatial distribution of water class (cation exchange code) for the analyzed samples. Fig. 14

reveals that in the southern part in the upstream direction of the study area and in Janzur, F and Fb water types have (+) code. This is due to Mg^{2+} dissolved from the carbonate rocks. Close to the Mediterranean shoreline in the dwonstream direction, 11 wells with (-) code, clearly pointing at cation exchange due to salinization, especially in Tajura coastal area. Large numbers of wells towards the north of the study area show (0), which falsely suggests cation exchange equilibrium; but, in this case, the decreased cation exchange parameter ({$Na^{+}+K^{+}+Mg^{2+}$} corrected for sea salt) compared to the fresh end member is indicating saltwater intrusion. It was also noticed that most of the wells with (+) code are F moderately hard, Fb hard to B very hard water with Ca/MgMix, MgCl or CaSO4 water types, while the B very hard CaCl type was noticed for most samples with equilibrium code. Most of
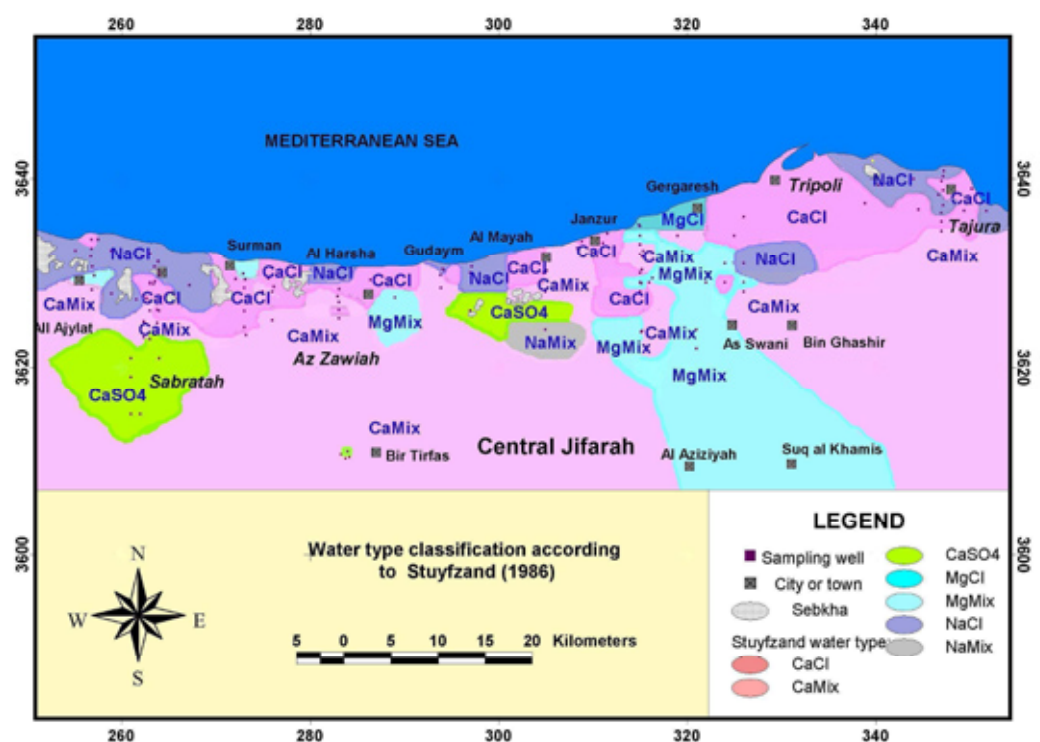

Figure 16. Distribution of water subtypes according to Stuyfzand (1986).
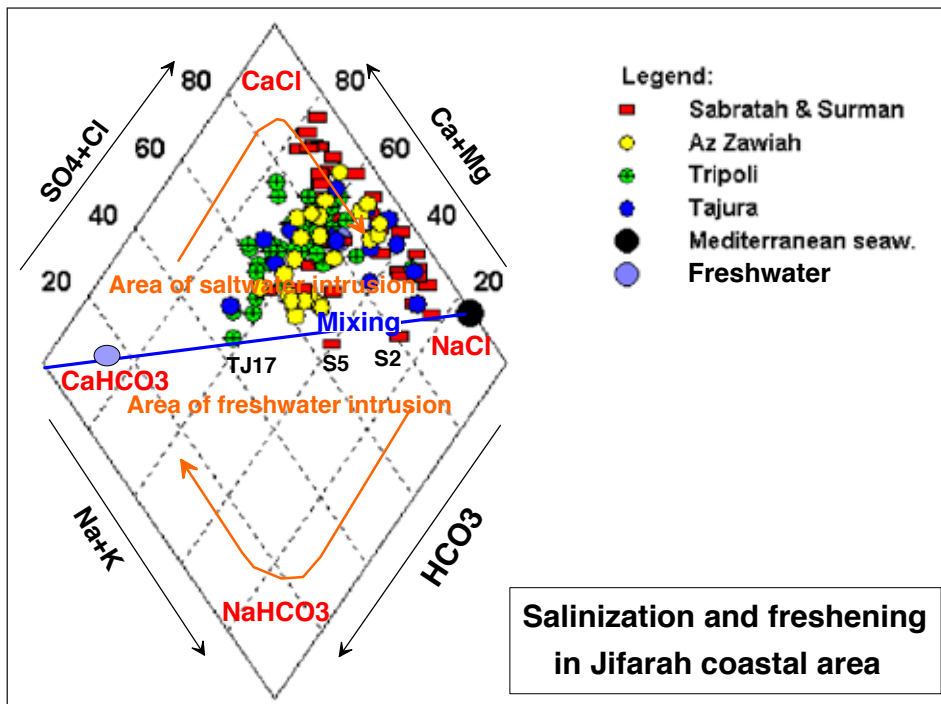
the wells with (-) code are Bs extremely hard NaCl water.

Subtype (ions prevailing):

The subtype is quite important to recognize the processes that have determined the water quality. Figure 15 represents the classification of water subtypes. Figure 16 is a map showing the spatial distribution of water subtypes, which reveals that most of shallow wells close to the shoreline have Brackish-saline extremely hard NaCl to Brackish very hard CaCl water. Some of shallow wells in Janzur are Fresh to Fresh-brackish Ca/MgMix with HCO_3^- as prominent anion, such as wells TJ16 and TJ7. In general, Ca/MgMix is found in the south (upflow), evolving to CaCl and NaCl downflow. In Sabratah, groundwater from the upper aquifer varies from $CaSO_4$ to Ca/MgMix in the south (upflow) to CaCl and NaCl close to the shoreline (downflow) and inland, where the cone of depression is formed.

Figure 17, representing salinization and freshening in the Piper diagram, reveals that all the analyzed samples are plotted in the part indicating salinization. Cation exchange is an important factor modifying groundwater quality and is one of the most important geochemical processes taking place in the upper Jifarah Plain aquifer. The region of the CaCl type water may be a leading edge of the seawater plume (Vengosh et al., 1991; Appelo & Postma, 1993; Jeen et al., 2001). Concluding, the water types are mainly F to Fb moderately hard, hard to very hard Ca/MgMix with HCO_3^- as dominant anion in the south (upstream), while in the north (downstream), they are evolving to B very hard CaCl and Bs extremely hard NaCl types towards the coast and in the large depression cones.

Another important aspect is the possible existence of evaporitic rocks intercalated in the aquifer rocks South of

Sabratah. In Sabratah area, the Fb hard $CaSO_4$ type is frequently found related to gypsum dissolution. The high salinity and relatively high concentrations of sulphate found in some samples taken from inland wells could be related to these saline precipitates. On the basis of currently available data, we cannot discard the possibility that a process of marine intrusion may be affecting areas of the aquifer close to these points, where the concentration of Cl⁻ is relatively high for many wells. Another process, in addition to the dissolution of evaporitic salts, and which could also contribute to the increased salinity of the aquifer, is the infiltration of waters having undergone evaporative concentration in the sebkhas, producing high SO_4^{2-} water.

5. Conclusion and summary

Dropping water tables have been recorded along the coast as a result of aquifer overexploitation. The aquifer is showing an increase in salinization, which has reached an alarming level in many places. The agricultural output is being impacted and damage to the top soil has taken place in several areas, especially in the Sabratah region. The hydrochemical interpretation indicates that dissolution of calcite, dolomite and/or Mg^{2+}- bearing calcite is an important process in most of the groundwaters. Stuyfzand classification clearly shows significant geochemical differences between the coast and the inland sector. The hydrochemical evolution of groundwater follows paths, from Ca/MgMix water types in the south via Mg/CaCl types to the NaCl type close to the sea. This pattern indicates that groundwater chemistry is changed by cation exchange reactions during the mixing process between freshwater and seawater. The NaCl and CaCl waters indicate a strong relationship with seawater. Ca/MgMix (HCO₃Cl) is probably a transitional type from freshwater

to saltwater. In the Sabratah area, the $CaSO_4$ type is found inland, pointing to gypsum dissolution.

A majority of the groundwater samples (80%) shows a composition that is indicative of seawater intrusion according to the Stuyfzand classification. A large number of the sampling points belong to the Brackish and Brackish-saline major type (Cl^- > 300 mg/l), and are very hard to extremely hard due to strong seawater admixture (with cation exchange code "–"or "0"). A lower number of samples are Fresh to Fresh-brackish and moderately hard to hard (cation exchange code "+"). The positive code is not indicating freshening, but is related to the origin of Mg^{2+}, mainly resulting from the freshwater end member (Mg^{2+}- containing carbonate was dissolved) rather than derived from seawater. For the majority of samples, the main subtype is CaCl, followed by Ca/MgMix (Ca/Mg-ClHCO_3) and NaCl subtypes. A few samples have a NaMix subtype, and show {Na + K + Mg}-surplus. The Cl^- concentrations and EC levels are highly positively associated. Lower ratios of Na/Cl than the seawater ratio indicate seawater encroachment. Of the coastal groundwaters, 61% exceed the recommended Cl^- value for standard drinking water (250 mg/l) and 26% have Cl^- greater than the highest admissible level of 600 mg/l. High salinity water with TDS values above 1500 mg/l needs careful management.

In conclusion, the salinization process in the Jifarah coast has primarily four origins. The first one is mainly due to seawater intrusion, which is mixed with the freshwater in the aquifer and reduces its quality. Groundwater in the western and southern coastal areas is heavily used for agricultural irrigation. Salinization of fresh groundwater is highly associated with continuous groundwater withdrawal.

The second origin of salinity is due to upconing of deep saline water, where the overexploitation of the aquifer causes the deeper and saline groundwater to rise. The third cause of salinity is due to dissolution of scattered sebkha deposits; this was observed in several wells. A fourth source includes the dissolution of gypsum intercalated within the lower aquifer formations south of Sabratah. Other sources include the salt concentration in the agricultural return flow and nitrate pollution. The irrigated water is mainly of groundwater origin and the salt concentration is increased from its initial value due to evapotranspiration. Furthermore, the lowering of the water table is forcing the infiltrated water to travel a larger distance through the soil, which will still increase evaporation, and thus salt concentration.

7. References

APHA (American Public Health Association)., 1985. Standard methods for the examination of water and wastewater. (éd.), *Greenberg A.E. (APHA), Trussell, R.R. & Clesceri, L.S.* American Public Health Association, Washington DC.

APPELO, C.A.J., 1994. Cation and proton exchange, pH variations, and carbonate reactions in a freshening aquifer. *Water Resources Research*, 30: 2793-2805.

APPELO, C.A.J., & POSTMA, D., 1993. Geochemistry, groundwater and pollution: Rotterdam, Netherlands, and Brookfield, Vermont, A. A. Balkema.

BARKER, A., NEWTON, R. & BITTRELL, S., 1998. Process affecting groundwater chemistry in a zone of saline intrusion into an urban sandstone aquifer. *Applied Geochemistry*, 13: 735-749.

DEMIREL, Z., 2004. The history and evaluation of saltwater intrusion into a coastal aquifer in Mersin, Turkey. *Journal of Environment Management*, 70: 275-282.

DGR (Direction Générale des Ressources en Eau)., 1995. *Annuaire d'exploitation des nappes phréatiques*. Ministère de l' Agriculture, Tunisia.

DIXON, W. & CHIWELL, B., 1992. The use of hydrochemical sections to identify recharge areas and saline intrusions in alluvial aquifers, Southeast Queensland, Australia. *Journal of Hydrology,* 135: 259-274.

DUQUE, C., CALVACHE, M.L., PEDRERA, A., MARTIN-ROSALES, W.M. & LÓPEZ-CHICANO, M., 2008. Combined time domain electromagnetic soundings and gravimetry to determine marine intrusion in a detrital coastal aquifer (Southern Spain). *Journal of Hydrology,* 349: 536-547.

EL MANSOURI, B., LOUKILI, Y. & ESSELAOUI, D., 2003. Mise en évidence et étude du phénomène de l'upconing dans la nappe côtière du Rharb (NW du Maroc), *Instituto Geológico y Minero de España (IGME), Madrid,* 84-7840- 470-8.

EL MOUJABBER, M., BOU SAMRA, B., DARWISH, T. & ATALLAH, T., 2006. Comparison of different indicators for groundwater contamination by seawater intrusion on the Lebanese coast. *Water Resources Management,* 20: 161-180.

FROHLICH, R.K., BAROSH, P.J. & BOVING, T., 2008. Investigating changes of electrical characteristics of the saturated zone affected by hazardous organic waste. *Applied Geophysics,* 64: 25-36.

GAALOUL, N., ALEXANDER, H. & CHENG, D., 2003. Hydrogeological and hydrochemical investigation of coastal aquifers in Tunisia-crisis in overexploitation and salinisation. *In: Second International Conference on Saltwater Intrusion and Coastal Aquifers -Monitoring, Modeling and Management*. Merida, Mexico, March 30-April 2, 2003.

GIMÉNEZ, E. & MORELL, I., 1997. Hydrogeochemical analysis of salinization processes in the coastal aquifer of Oropesa (Castellon, Spain). *Environmental Geology,* 29:118-131.

IRC (Industrial Research Centre), 1995. Geological card of Jifarah Plain, edition 2. *Great Socialist People's Libyan Arab Jamahiriyah*. Tajura, Libya.

JEEN, S.W., KIM, J.M., KO, K.S., YUM, B.W. & CHANG, H.W., 2001. Hydrogeochemical characteristics of groundwater in a Midwestern coastal aquifer system, Korea. *Geosciences,* 5: 339-348.

JONES, B.F., VENGOSH, AVNER, ROSENTHAL, ELIYAHU, YECHIELI & YOSEPH., 1999. Geochemical investigations. In Bear, Jacob et al. (eds), *Seawater intrusion in coastal aquifers-Concepts, methods and practices. Dordrecht, The Netherlands, Kluwer Academic Publishers,* 51-71.

KREITLER, C.W. & RICHTER, B.C., 1993. *Geochemical Techniques for Identifying Sources of Groundwater Salinization*. Boca Raton, Florida: C.K., Smoley.

MAGARITZ, M. & LUZIER, J.E., 1985. Water-rock interactions and seawater-freshwater mixing effects in the coastal dune aquifer, Coos Bay, Oregon. *Applied Geochemistry,* 49: 2515-2525.

MAHESHA, A. & NAGARAJA, S.H., 1996. Effect of natural recharge on seawater intrusion in coastal aquifers. *Hydrogeology Journal,* 174: 211-220.

MERCADO, A., 1985. The use of hydrogeochemical patterns in carbonate sand and sandstone aquifers to identify intrusion and flushing of saline waters. *Ground Water,* 23: 635-645.

MORELL, I., GIMÉNEZ, E. & ESTELLER, M.V., 1996. Application of principal components analysis to the study of salinization on the Castellon Plain (Spain). *Geosciences,* 177: 161-171.

NADLER, A., MAGARITZ, M. & MAZOR, E., 1981. Chemical reactions of seawater with rocks and freshwater. Experimental and field observations on brackish waters in Israel. *Applied Geochemistry,* 44: 879-886.

PALLAS, P., 2006. Mathematical modeling of the Tunisian-Libyan Jifarah Aquifers. Final report. part 1. *General Water Authority (GWA), Tripoli, Libya*.

PULIDO-LEBOEUF, P., 2004. Seawater intrusion and associated processes in a small coastal complex aquifer (Castell de Ferro, Spain). *Applied Geochemistry,* 19: 1517-1527.

REVELLE, R., 1941. Criteria for recognition of sea water in groundwaters. *Transactions of the American Geophysical Union,* 22: 593-597.

SANCHEZ MARTOS, F., PULIDO BOSCH, A. & CALAFORRA, JM., 1999. Hydrogeochemical processes in an arid region of Europe (Almeria, SE Spain). *Applied Geochemistry,* 14: 735-745.

STAMATIS, G. & VOUDOURIS, K., 2003. Marine and human activity influences on the groundwater quality of southern Korinthos area (Greece). *Hydrological Processes,* 17: 2327-2345.

STUYFZAND, P.J., 1986. A new hydrogeochemical classification of water types: principles and application to the coastal dunes aquifer system of the Netherlands. *Proceedings 9th Sea Water Intrusion Meeting (SWIM), Delft (The Netherlands),* 641-656.

STUYFZAND, P.J., 1993. Hydrochemistry and hydrology of the coastal dune area of the Western Netherlands. *PhD dissertation, Free university (VU), Amsterdam*, 90-74741-01-0, 366 p.

SUKHIJA, B.S., VARMA, V.N., NAGABHUSHANAM, P. & REDDY, D.V., 1996, Differentiation of paleomarine and modern seawater intruded salinities in coastal line groundwater (of Karaikal and Tanjavur, India) based on inorganic chemistry, organic biomarker fingerprints and radiocarbon dating. *Journal of Hydrology,* 174: 173-201.

TODD DK., 1959. *Ground water hydrology.* Wiley, New York.

VENGOSH, A., STARINSKY, A., MELLOUL, A., FINK, M. & ERLICH, S., 1991. Salinization of the coastal aquifer water by Ca-chloride solutions at the interface zone, along the Coastal Plain of Israel. *Hydrological Service, Jerusalem*.

WALRAEVENS, K. & VAN CAMP, M., 2005. Advances in understanding natural groundwater quality controls in coastal aquifers, *18 Sea Water Intrusion Meeting (SWIM). Cartagena 2004, Spain*, 451-460.

WHO (World Health Organization)., 1984. *Guidelines for Drinking-Water Quality*. Vol. 2. Health criteria and other supporting information, Geneva, 717 p.